# Effect of finite size on the Kosterlitz-Thouless transition in two-dimensional arrays of proximity-coupled junctions

S. T. Herbert
*Department of Physics, Xavier University, Cincinnati, Ohio 45207*

Y. Jun* and R. S. Newrock
*Department of Physics, University of Cincinnati, Cincinnati, Ohio 45221*

C. J. Lobb
*Center for Superconductivity, Department of Physics, University of Maryland, College Park, Maryland 20742*

K. Ravindran, H.-K. Shin,† D. B. Mast, and S. Elhamri
*Department of Physics, University of Cincinnati, Cincinnati, Ohio 45221*

(Received 27 August 1997)

We have investigated the Kosterlitz-Thouless (KT) transition in a series of proximity-coupled Josephson junction arrays of varying widths. Our results indicate that the KT transition in any experimentally realizable sample is almost always obscured by the presence of thermally generated, finite-size-induced free vortices. While the existence of these finite-size-induced free vortices has been known for some time, our work suggests that they are much more prevalent and thus have a far greater effect on the transition than had been previously thought. As a consequence of this, the vortex-unbinding transition temperature $T_{KT}$ may not occur when the experimentally measured current-voltage exponent $a(T)=3$, but in fact may occur at significantly higher temperatures. We present a detailed picture of these finite-size effects applied specifically to arrays, but which may have implications for other two-dimensional systems. [S0163-1829(98)08101-6]

## I. INTRODUCTION

In 1979 Beasley, Mooij, and Orlando[1] (BMO) suggested that the Kosterlitz-Thouless (KT) transition may be observable in two-dimensional (2D) superconducting systems. They showed that under certain conditions the relevant penetration depth $\lambda_\perp=\lambda^2/d$ (where $\lambda$ is the bulk penetration depth and $d$ the sample thickness) could reach lengths comparable to the sample size. This would allow vortices to interact logarithmically[2] over the entire sample, a necessary condition for a KT transition to be seen.

In the more than one and a half decades of investigation since that time, many groups have reported evidence for KT behavior in a variety of 2D superconducting systems, including high-resistance granular films and arrays of Josephson junctions.[3] Recently, a whole new class of systems, the cuprate superconductors, has been suggested as exhibiting a KT transition.[4] While many of the features of the KT transition have been reported in these systems, many discrepancies remain to be explained.

One such discrepancy, which will be the focus of this paper, involves the current-voltage ($I$-$V$) characteristics of a 2D superconductor. The KT theory predicts power-law behavior in the $I$-$V$ curves (i.e., $V\propto I^{a(T)}$) for temperatures at and below the KT transition temperature $T_{KT}$. Precisely at $T_{KT}$, the $I$-$V$ exponent $a(T)$ is predicted to be 3, with increasing values as the temperature is lowered. This power law behavior should persist to the limit of zero current. Experimental $I$-$V$ curves, however, very often exhibit deviations from pure power-law behavior towards an Ohmic slope $[a(T)=1]$ at very low currents, precisely where they should *not* occur. Often these deviations are dismissed as resulting from a small remnant magnetic field, or from instrumentation or current noise.

In this paper we present evidence that deviations of the $I$-$V$ curves from pure power-law behavior below the transition temperature are caused by the presence of thermally generated free vortices that are not the result of the KT thermal unbinding mechanism, but rather result from the sample being of finite size. The existence of finite-size-induced free vortices was first noted by KT (Ref. 5) and BMO,[1] and later by Minnhagen[6] for a 2D Coulomb gas. It has often been assumed, however, that the number of finite-size-induced vortices is small and hence would have few experimentally observable consequences. Our analysis suggests that this is not the case. Here we present a more detailed picture of finite-size effects applied specifically to arrays of Josephson junctions, but which has broad implications for other 2D systems. Since the KT picture involves the transition from a low-temperature state in which only paired vortices exist to a high-temperature state in which free vortices occur, we would argue that the existence of free vortices below $T_{KT}$ means that the KT transition does not take place in the strict sense of a true phase transition (i.e., no free vortices below $T_{KT}$ and free vortices above $T_{KT}$).

This strict interpretation of the definition of a phase transition does not mean, however, that the KT vortex-unbinding *mechanism* does not occur and is not observable. If we ignore the deviations at low current and simply extract the $I$-$V$ exponents from the power-law portion of the $I$-$V$ curves (which generally has been done for many years), we fre-

 © 1998 The American Physical Society

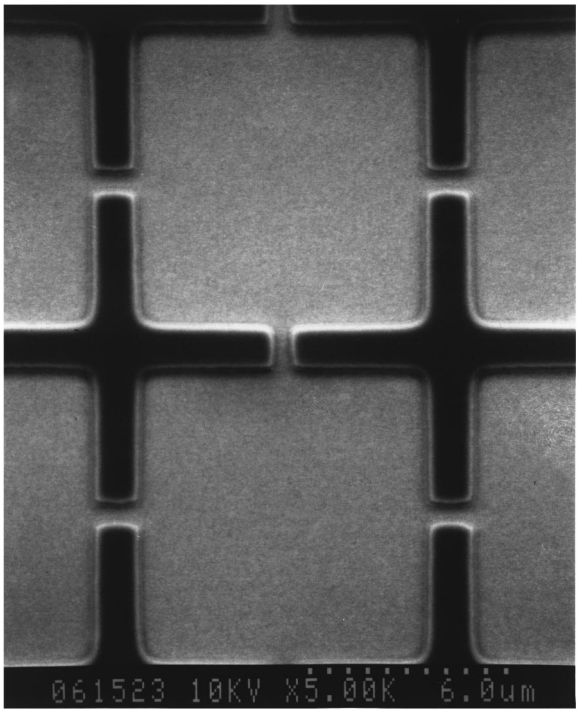


FIG. 1. Scanning electron micrograph of a typical array showing the superconducting cross geometry.

quently obtain the expected jump in $a(T)$ from 1 to 3 as predicted by the KT model. Despite the presence of this seemingly unambiguous signpost of the KT transition [i.e., the jump in $a(T)$], our analysis indicates that the significant presence of finite-size-induced vortices may mask the power-law exponent, making the simple approach to analyzing the $I$-$V$ curves problematic and leading to an incorrect estimate of the transition temperature.

The remainder of the paper will be organized as follows: In Sec. II we present data from a systematic study of proximity-coupled Josephson junction arrays to examine the effect that finite array size has on the $I$-$V$ characteristics. In Sec. III we briefly review the relevant details of the KT theory, and in Sec. IV we derive an expression for the free-vortex density in finite-sized arrays. We discuss the experimental consequences of the free-vortex density in Sec. V and apply the results to experimental data on finite-sized arrays in Sec. VI. Finally, we summarize the overall conclusions of the paper in Sec. VII.

## II. EXPERIMENTAL RESULTS ON FINITE-SIZED ARRAYS

Our measurements were performed on a series of proximity-coupled Josephson junction arrays consisting of a square lattice of niobium crosses decorating a continuous gold film (see Fig. 1). The cross arms were nominally 1 $\mu$m wide with a gap distance between adjacent cross arms of approximately 0.7 $\mu$m; the lattice constant for all the arrays was 10 $\mu$m. The arrays were 300 crosses long in the direction of the current, but varied in width (i.e., transverse to the current), with the samples studied being $W=300$, 200, 100, 75, 50, 20, 15, 10, and 3 crosses wide.[7] Transport measurements (dc) were made by applying a square-wave excitation current ($f=13$ Hz) and synchronously detecting the voltage using a transformer-coupled lock-in amplifier. The noise floor of the system was approximately 0.5 nV. The temperature was controlled to better than $\pm 1$ mK and the Earth's magnetic field was canceled using a small superconducting solenoid, yielding an ambient magnetic field of less than 0.5 mOe. All measurements were taken inside a grounded, shielded screened room.

In Fig. 2 we show the $I$-$V$ characteristics for four arrays of widths 300, 75, 50, and 20 crosses. The $I$-$V$ curves for each sample are shown at various temperatures, spaced roughly 0.1 K apart. As the data are plotted logarithmically, a straight line denotes power-law behavior and the slope of the curve is the $I$-$V$ exponent $a(T)$. An $I$-$V$ curve with a slope of one indicates Ohmic behavior. The heavy black line in each plot indicates a slope of 3, which, in the KT theory,[8,9] is the zero-current slope of the $I$-$V$ curve at the transition temperature $T_{\mathrm{KT}}$. However, several of the $I$-$V$ curves in Fig. 2 identified with the heavy black line display a ''tail'' at low currents which deviates from a slope of 3. In addition, we will show in Sec. VI that a measured slope of 3 in the data does not necessarily imply that one is *at* the KT transition temperature or even that such a transition exists. Thus we are reluctant to label this temperature the KT transition temperature. For the purposes of discussion, however, it will be useful to define $T_{a=3}$ as the temperature at which the power-law portion of the $I$-$V$ curve displays a slope of 3. (In the absence of finite-size effects, we would normally identify $T_{a=3}=T_{\mathrm{KT}}$.) For the four arrays shown here, $T_{a=3}$ is measured to be 2.55, 2.48, 2.32, and 3.22 K for the $W=300$, 75, 50, and 20 arrays, respectively.

Focusing on the $I$-$V$ curves at and below $T_{a=3}$, the data for the $W=300$ array exhibit behavior indicative of a KT transition: Ohmic behavior at high temperatures followed by a sudden jump to power-law behavior with a slope of 3 at the transition temperature. The power-law slopes of 3 or greater arise out of the noise floor and persist over several decades, with the slope increasing as the temperature is decreased. Note, however, that the data for the $I$-$V$ curve at $T_{a=3}$ begins to deviate from a strict power law at the lowest currents, bending towards an Ohmic (linear) slope. Although this variation is slight, deviations of this kind or much greater are usually observed in 2D arrays[10] and are often dismissed as resulting from a small remnant magnetic field or instrumentation noise. By contrast in our arrays, where the remnant field is small and careful filtering has been done, we believe that these deviations indicate the presence of additional free vortices in the array that are not created via the KT vortex-unbinding process, but result from the arrays being of finite extent.

The deviation from power-law behavior appears to be significant (if small) only at $T_{a=3}$ for the $W=300$ array; for lower temperatures, the $I$-$V$ curves are still power-law-like to the lowest measurable currents. As the arrays become more narrow, however, these deviations persist to lower temperatures and become more pronounced. The $W=75$ array data show a significant tail, nearly Ohmic in slope, for $I$-$V$ curves from $T_{a=3}$ to the lowest temperature measured. The $W=50$ array shows data similar in character to the $W=75$ array, but the tail is less dramatic (i.e., less obviously Ohmic) and disappears at the lowest temperatures rather than persist-

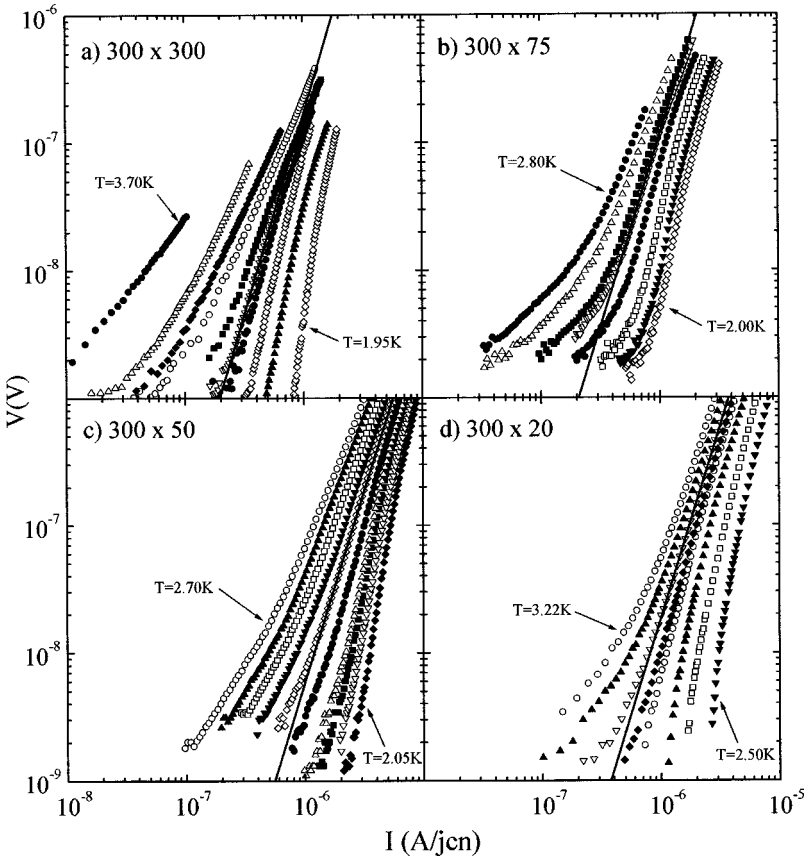


FIG. 2. Current-voltage characteristics as a function of temperature for four arrays of width (a) 300 crosses, (b) 75 crosses, (c) 50 crosses, and (d) 20 crosses. Each array is 300 crosses long. The current is divided by the width $W$ of each array (in units of amperes/junction). The solid line in each plot indicates a slope of 3.

ing as it does in the $W=75$ array. The different behavior of the Ohmic tails in the $W=75$ and 50 arrays (indeed, between any two arrays) will be explored more fully in Sec. V.

We could proceed then, as has been commonly done, by ignoring the tail region of the $I$-$V$ curves and simply measure the slope of the power-law region. Figure 3(a) shows the measured $I$-$V$ exponents from the *power-law region* of the curve as a function of temperature for the $W=300$, 75, and 50 arrays. Each array exhibits a significant jump in $a(T)$ from 1 to 3, but $T_{a=3}$ is suppressed and the transition is broadened as the arrays become narrower. This effect has been observed previously in randomly disordered arrays near the percolation threshold[10] and is a result of the arrays not being fully renormalized as the KT scale length decreases with decreasing width.[7,13] If instead we measure each $I$-$V$ exponent in the limit of zero current (as the KT prescription dictates), we obtain quite a different picture [Fig. 3(b)]. The $W=300$ array still shows a significant jump, though suppressed slightly in temperature. No jump occurs for the $W=75$ and 50 arrays. The $W=50$ array shows only a gradual rise that seems to continue unchanged through $a(T)=3$, while the $W=75$ array displays essentially Ohmic behavior to the lowest temperature measured.

Figures 3(a) and 3(b) point out a long-standing quandary concerning where to measure the correct $I$-$V$ exponent. We believe that the deviations from pure power-law behavior below $T_{\mathrm{KT}}$ are not the result of data collection conditions, but are intrinsic to the finite-sized nature of the sample. As such, ignoring the Ohmic tail region of the $I$-$V$ curve and measuring the power-law region alone can lead to potentially misleading and incorrect values of $a(T)$ and, hence, a misinterpretation of the KT transition. We will return to this issue in Sec. VI.

The $I$-$V$ curves of Figs. 2(b) and 2(c), along with the corresponding $a(T)$ data in Fig. 3(b), are reminiscent of recent measurements by Repaci *et al.*[11] in which they reported the absence of a KT transition in single unit-cell-thick $YBa_2Cu_3O_x$ (YBCO) films. In that work they show $I$-$V$ curves with power-law slopes greater than 3 that have significant Ohmic tails. They argue, in a manner consistent with ours, that the Ohmic tail results from a thermal population of free vortices. The absence of the KT transition in their YBCO films may not be surprising since the cuprate superconductors are not in the dirty limit and, as such, should display little enhancement of the bulk penetration depth. In contrast, Josephson junction arrays have long been thought to display a KT transition.

Finally, the $W=20$ array [Fig. 2(d)] shows power-law $I$-$V$ curves with an Ohmic tail at and just below $T_{a=3}$, but the $I$-$V$ curves quickly turn over to a downward curvature as the temperature is lowered. In the $W=15$ array (not shown), the $I$-$V$ curves are concave downward with no trace of the power-law behavior seen in wider arras. In fact, the $I$-$V$ characteristics of the $W=15$ array strongly resemble the $I$-$V$ characteristics of a single junction. Thus the $W=20$ array is the narrowest array in which the experimental signature of

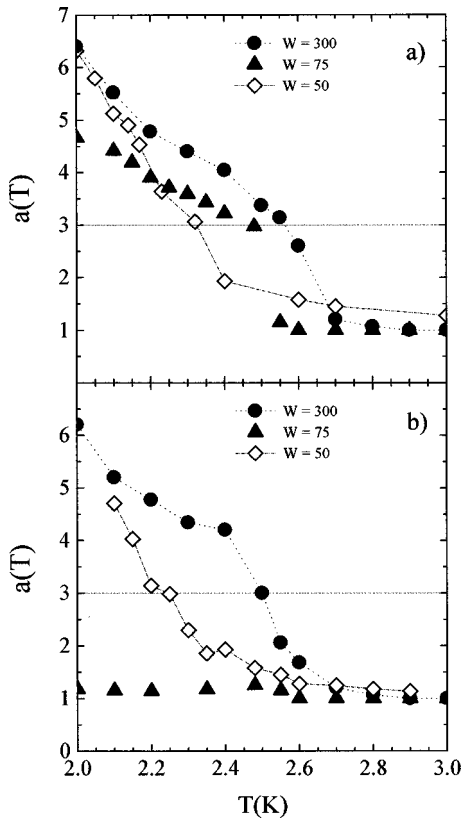


FIG. 3. $a(T)$ vs $T$ for the $W=300$, 75, and 50 arrays (a) as measured from the power-law regime only and (b) as measured in the limit of low applied current.

vortex unbinding, the power-law $I$-$V$ characteristic, can be observed. This result is consistent with a simple thermodynamic argument. (See the Appendix.) The details of this will be explored in a future paper.[7]

### III. REVIEW OF KT THEORY

In order to discuss the origin of the Ohmic tail, it is instructive to review the various length scales important to the KT transition. It is well known that the KT transition is only rigorously defined for an infinite 2D system where the vortices interact logarithmically.[1,5,6] In two dimensions, the perpendicular penetration depth $\lambda_\perp$ gives the length scale below which the screening current density varies[2] as $1/r$; for $r>\lambda_\perp$, the screening current density varies as $1/r^2$. In order to assure that vortices will interact logarithmically over all lengths, $\lambda_\perp$ must be larger than the sample size $L$, so that we must satisfy the condition $\lambda_\perp \gg L \to \infty$ to be in the thermodynamic limit.

Above the transition temperature $T_{\mathrm{KT}}$, an important parameter is the vortex correlation length $\xi_+(T)$, which defines the size of the fluctuations associated with the phase transition or, alternatively, gives the average distance between free vortices. For 2D arrays, $\xi_+(T)$ is[12]

$$\xi_+(T)=C_1 a_0 \exp\{[C_2/(T'-T'_{\mathrm{KT}})]^{1/2}\}, \tag{1}$$

where $C_1$ and $C_2$ are of order unity and $a_0$ is the lattice constant of the array. A dimensionless temperature $T'=2ek_BT/\hbar i_c(T)$ is used to remove the strong temperature dependence of the single-junction critical current $i_c(T)$ from the temperature dependence of the underlying phase transition.

As $T$ approaches $T_{\mathrm{KT}}$ from above, $\xi_+$ increases, meaning that, on average, free vortices are separated by greater distances. Vortices separated by distances less than $\xi_+$ are, on average, bound. In the presence of a *small* external excitation current, the free vortices will move, creating a flux-flow resistance, and hence we see an Ohmic response in the current-voltage characteristics. As $T$ is decreased further, $\xi_+$ continues to grow, more and more vortices become bound in pairs, and the magnitude of the flux-flow resistance is reduced. At $T_{\mathrm{KT}}$, $\xi_+$ becomes infinite, meaning that all vortices are bound and the resistance disappears; a true zero-resistance state occurs in the limit of zero current.

A finite applied current will unbind the most weakly bound vortices (those ''infinitely'' far apart), leading to dissipation, so that even though a true zero-resistance state exists, it also has zero critical current. This current-induced vortex unbinding is a non-Ohmic, power-law process [$V(I) \propto I^{a(T)}$ where $a(T)>3$]; no Ohmic behavior should exist below $T_{\mathrm{KT}}$ at sufficiently low current densities. At $T_{\mathrm{KT}}$ the KT theory specifies that the exponent of the power law is $a(T_{\mathrm{KT}})=3$, and we have the so-called ''universal jump'' in the superfluid density—since for sufficiently small currents an Ohmic regime exists just above $T_{\mathrm{KT}}$, a plot of $a(T)$ vs temperature will show a jump from 1 to 3 at $T_{\mathrm{KT}}$. Note the emphasis on small currents. Sufficiently large currents can unbind pairs, leading to a non-Ohmic $I$-$V$ curve even above $T_{\mathrm{KT}}$ [although in this regime $1<a(T)<3$].

One important complication for ''infinite'' samples involves the renormalization of the vortex-antivortex interaction. This is dealt with extensively elsewhere,[13] and so we will simply sketch the results here. For all temperatures above zero, there will exist bound vortex-antivortex pairs separated by a range of distances, both large and small. Vortex pairs separated by large distances will be screened by smaller, polarizable pairs that exist between a particular bound vortex and antivortex. The effect is to reduce the strength of the interaction that binds pairs separated by the greatest distances. These weakly bound pairs have the greatest effect on the measurements, in terms of the temperature and current dependence. This renormalization of the interaction is accounted for by introducing into the expression for the vortex interaction potential [$U(r)=2\pi E_j(T)\ln(r/a_0)$] a length-dependent effective dielectric constant $\epsilon(r)$, so that $U(r)$ becomes

$$U(r)=\int_{r'=a_0}^{r'=r} \frac{2\pi E_j(T)}{\epsilon(r')}\, d(\ln r'), \tag{2}$$

where $E_j(T)=\hbar i_c(T)/2e$ is the bare or unrenormalized vortex coupling energy and $r$ is the vortex separation. The vortex interaction potential is often written $U_P(r)=2\pi E_j^*(T)\ln(r/a_0)$, where $E_j^*(T)$ is known as the renormalized coupling energy. At infinite distances, intervening vortex pairs of all sizes modify the vortex interaction and the interaction is fully renormalized; the essential features of the KT transition, however—the universal jump and the square-root cusp in the current-voltage exponent—are preserved.

Any experimental system will be of finite size and the maximum separation between bound vortices will be limited by the sample size. In addition, only vortex pairs separated by distances less than the sample size can participate in the screening $\epsilon(r)$ and the transition will not be fully renormalized. The effect of finite sample size on the renormalization of the transition can be dealt with in a calculable way, and this has been done by Kadin, Epstein, and Goldman.[13] As the sample size is reduced from infinity, the universal jump becomes broadened and $a(T)$ no longer jumps from 1 to 3 at the transition, but rather exhibits a more gradual crossover. This effect has been observed and verified experimentally[10] and is *not the effect that we will discuss here*.

## IV. FINITE-SIZE CUTOFF

Another more serious effect of finite sample size is the existence of thermally generated free vortices in the array *at all nonzero temperatures*. This is in contrast to the true KT transition where there are no thermally generated free vortices for $T \leqslant T_{\mathrm{KT}}$.

In a finite array the free energy to create a single vortex is finite for all temperatures. The probability of creating a free vortex is given by $P_f \sim \exp[-F(T)/k_B T]$, where $F(T)$ is the free energy of a vortex. The number of possible places for a vortex of core size $a_0$ to exist in a square array of size $L^2$ is $L^2/a_0^2$ so that we may write the positional entropy as $S(L) = k_B \ln(L^2/a_0^2)$. Hence the free energy is $F(T) = U(L) - TS(L) = \pi E_J^* \ln(L/a_0) - k_B T \ln(L^2/a_0^2)$. For the probability we then have

$$P_f \sim \exp\left\{ \frac{-1}{k_B T} \left[ \ln\left(\frac{L}{a_0}\right)^{\pi E_J^*} - \ln\left(\frac{L}{a_0}\right)^{2k_B T} \right] \right\}. \tag{3}$$

Simplifying,

$$P_f \sim \left(\frac{L}{a_0}\right)^{-\pi E_J^*/k_B T} \left(\frac{L}{a_0}\right)^2 \sim \left(\frac{L}{a_0}\right)^{2-2T_{\mathrm{KT}}/T}, \tag{4}$$

where the final form follows from $k_B T_{\mathrm{KT}} = \pi E_J^*(T_{\mathrm{KT}})/2$. For temperatures below $T_{\mathrm{KT}}$, $\pi E_J^*/k_B T > 2$ and hence $P_f = 0$ for an infinite specimen. For a finite sample, however, $P_f$ is *never* zero for nonzero temperatures. At $T_{\mathrm{KT}}$, Eq. (4) tells us that the probability of creating a single free vortex is of order 1, regardless of the sample size. However, as we shall show below, for an infinite sample the free-vortex *density* is zero at $T = T_{\mathrm{KT}}$.

Equation (4) does not give us the actual free-vortex density needed to compute a flux-flow resistance. The free-vortex density $n_f'$ for a finite sample will be proportional to the probability of creating a free vortex, and so we use Eq. (4) to write

$$n_f' = \beta_1 \left(\frac{L}{a_0}\right)^{2-2T_{\mathrm{KT}}/T}, \tag{5}$$

where $\beta_1$ is a parameter to be determined (with dimensions of inverse area).

We may obtain another expression for the finite-sized free-vortex density *above* $T_{\mathrm{KT}}$ in the following manner. For a KT transition in an infinite sample, $n_f = b\xi_+^{-2}(T)$ for $T > T_{\mathrm{KT}}$ and $n_f = 0$ for $T \leqslant T_{\mathrm{KT}}$. (Note that here $b$ is a constant.) Using a finite-size scaling assumption, we may write,

$$n_f' = \frac{b}{\xi_+^2(T)} f(L/\xi_+), \tag{6}$$

where $f(L/\xi_+)$ is a scaling function to be determined. Since $\xi_+$ diverges at $T_{\mathrm{KT}}$, but $n_f' = 0$ only for $L = \infty$, Eq. (6) implies $f(L/\xi_+) = \beta_2(\xi_+/L)^2$ for $L \ll \xi_+$. (Here $\beta_2$ may in fact be temperature dependent.) Thus, at $T_{\mathrm{KT}}$, Eq. (6) becomes

$$n_f'(T = T_{\mathrm{KT}}) = \frac{b\beta_2(T)}{L^2}. \tag{7}$$

Comparing Eqs. (5) and (7) at $T = T_{\mathrm{KT}}$ gives $\beta_1 = b\beta_2(T)/L^2 = \beta(T)/L^2$ (where $\beta \equiv b\beta_2$), and Eq. (5) becomes

$$n_f' = \frac{\beta(T)}{a_0^2} \left(\frac{L}{a_0}\right)^{-\pi E_J^*/k_B T}. \tag{8}$$

Note that for an infinite sample the free-vortex density $n_f'$ goes to zero at $T_{\mathrm{KT}}$ as it should. The parameter $\beta(T)$ can be determined by a rigorous calculation of the energy of a vortex pair in equilibrium with an externally applied current. This treatment yields[14] $\beta(T) \cong \beta_0 \exp(-\pi E_J^*/k_B T) = \beta_0 \exp(-\pi/T')$, where $\beta_0$ may be taken as constant for small currents.

The previous analysis applies to finite-sized samples for which $\lambda_\perp \gg L > a_0$. A similar analysis can be done for the case in which $\lambda_\perp$ is smaller than the sample size, that is, when $L > \lambda_\perp > a_0$. In this case it is possible for vortices to exist in the sample that are separated by more than $\lambda_\perp$ and, hence, are not logarithmically bound. Thus $\lambda_\perp$, rather than $L$, becomes the relevant length scale in the free energy to create a single vortex, and we replace $U(L)$ with $U(\lambda_\perp) = \pi E_J^* \ln(\lambda_\perp/a_0)$ in Eq. (3). We can thus write a more general expression for the finite-size-induced free vortex density as

$$n_f' = \frac{\beta_0}{a_0^2} e^{-\pi E_J^*/k_B T} \left(\frac{\mathcal{L}}{a_0}\right)^{-\pi E_J^*/k_B T}, \tag{9}$$

where $\mathcal{L} \equiv \min\{L, \lambda_\perp\}$ and we have substituted in the expression for $\beta(T)$. While it is often assumed that $\lambda_\perp$ is larger than the sample size, the actual value is highly dependent on individual sample characteristics. For proximity-coupled arrays, $\lambda_\perp$ varies as $1/i_c(T)$, where $i_c(T)$ depends exponentially on the temperature;[12] weakly coupled arrays with smaller single junction critical currents will have larger perpendicular penetration lengths than strongly coupled arrays. As the temperature is lowered from above $T_{\mathrm{KT}}$, it is quite possible for an array sample to have $\lambda_\perp$ cross over and become smaller than the sample size near the KT vortex-unbinding temperature. This crossover will be reflected in the free-vortex density $n_f'$.

We pause here to clarify the distinction between the free-vortex density $n_f$ as normally used in a KT context and $n_f'$ as defined in Eq. (9). The free-vortex density $n_f$ refers to ther-

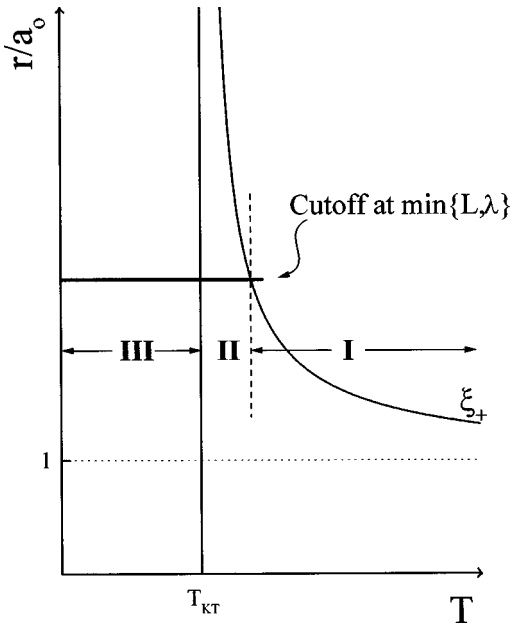


FIG. 4. Diagram indicating the temperature dependence of the KT coherence length $\xi_+$ and the different regions of the transition for an array of finite width.

mally unbound free vortices generated via the KT vortex-unbinding mechanism. It is nonzero only above $T_{\mathrm{KT}}$, and is technically applicable only in the thermodynamic limit. In contrast, $n_f'$ refers to all thermally generated free vortices, those generated via the KT vortex-unbinding mechanism above $T_{\mathrm{KT}}$ *and* those generated by finite-size effects at all finite temperatures. Thus $n_f'$ is never zero for any finite-sized sample, except at zero temperature.

## V. EXPERIMENTAL CONSEQUENCES

The KT vortex-unbinding transition occurs in samples where $\lambda_\perp > L \gg a_0$. Thus the finite size of $L$, $\lambda_\perp$, or both, and the resulting finite-size-induced free vortices will have a profound effect on experimental observations. Figure 4 illustrates the finite-sized unbinding mechanism. In region I temperatures are sufficiently above $T_{\mathrm{KT}}$ that vortex-antivortex pairs are created easily with average separations that are large compared to the lattice constant $a_0$. The KT correlation length $\xi_+$ is small in this regime (on the order of $a_0$) so that all but the closest pairs are unbound. In this regime effects of finite-sized-induced vortices are not observable since all vortex pairs are unbound via the KT mechanism anyway. Thus $I$-$V$ curves for temperatures in region I follow the predicted KT behavior.

As the temperature is lowered toward $T_{\mathrm{KT}}$, $\xi_+$ grows quickly, eventually meeting and exceeding the cutoff length scale $\mathcal{L} \equiv \min\{L, \lambda_\perp\}$ (region II). For ''infinite'' samples, vortices separated by less than $\xi_+$ should be bound, while vortices separated by distances greater than this length remain unbound, but will eventually *become* bound as $T$ decreases. The existence of the cutoff, however, means that the free vortex density $n_f'(T)$ will have a temperature dependence as given in Eq. (9). In practice, the $I$-$V$ curves in region II will strongly resemble the regular KT behavior: an Ohmic region at the lowest currents and power-law behavior with a slope less than 3 at higher currents. The major difference is that the Ohmic region will have a higher resistance resulting from the presence of the finite-size-induced vortices. While the $I$-$V$ curves could in principle be analyzed to extract this excess resistance, this would require an exact knowledge of $n_f$, which is difficult to obtain.

The most profound and easily observed effect of finite-size-induced free vortices occurs in region III, at and below $T_{\mathrm{KT}}$. Here $n_f$ becomes zero, while $n_f'$ remains nonzero. This results in $I$-$V$ curves with a low-current Ohmic tail below the nominal $T_{\mathrm{KT}}$ (or $T_{a=3}$), which can be clearly seen in Fig. 2 for our $W = 75$, 50, and 20 samples. The observed tail may not in fact have a slope of 1, but may appear as a deviation from pure power-law behavior towards Ohmic behavior; however, it must eventually have a slope of 1 at low enough current. The exact slope of the tail will depend on the voltage resolution of the measurement apparatus, the value of $n_f'$, and the coupling energy of the array which defines the KT unbinding temperature. Since the KT transition involves the establishment of quasi-long-range order resulting from the disappearance of all free vortices, the presence of free vortices destroys the phase transition in a strict sense, even though the KT vortex-unbinding mechanism may still be in evidence. In addition, the free vortices obscure the signatures of the KT vortex-unbinding mechanism by modifying the apparent slopes of the $I$-$V$ curves, as will be shown below.

## VI. COMPARISON WITH EXPERIMENT

The KT vortex-unbinding mechanism in the thermodynamic limit ($\lambda_\perp, L \to \infty$) gives rise to $I$-$V$ curves below $T_{\mathrm{KT}}$ that have a power-law dependence. The temperature dependence of the power-law exponent $a(T)$ below $T_{\mathrm{KT}}$ was predicted to be[8,12,15]

$$a(T) = \frac{\pi E_J(T)}{k_B T \epsilon_c} + 1 = \frac{\pi}{T' \epsilon_c} + 1, \tag{10}$$

where $T'$ is the reduced temperature and $\epsilon_c$ is the fully renormalized value of the dielectric constant just below the transition. Minnhagen *et al.*[16] have predicted a slightly different form

$$a(T) = \frac{2\pi E_J(T)}{k_B T \epsilon_c} - 1 = \frac{2\pi}{T' \epsilon_c} - 1, \tag{11}$$

and recent measurements on both conventional proximity-coupled arrays and high-$T_c$ weak-link arrays have shown better agreement with this expression.[17] We will thus use the Minnhagen result in the ensuing discussion; we note they are equivalent at $T = T_{\mathrm{KT}}$. (The results of this section do not depend explicitly on which model we use: however, the Minnhagen model seems to yield better results.)

Finite-size-induced free vortices will contribute a flux-flow voltage of the form $V = a_0^2 r_n n_f' I \equiv R' I$ in addition to the usual KT voltage characteristics. The total voltage signal will approximately be the sum of a power-law signal and a flux-flow resistance signal or

$$V = [\alpha_1 I^{a(T)} + \alpha_2 (a_0^2 r_n n_f') I], \tag{12}$$

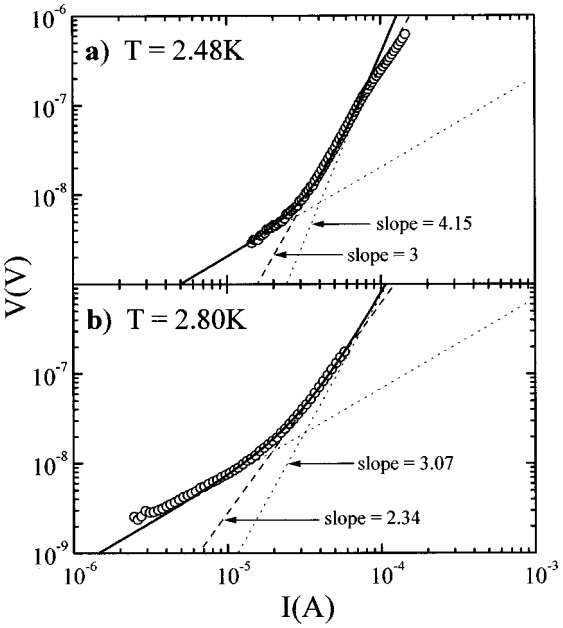


FIG. 5. $I$-$V$ curves from the $W=75$ array at (a) $T=2.48$ K and (b) $T=2.80$ K. Circles show actual data, and solid lines show the simulated $I$-$V$ curve at each temperature. The dotted lines show the power-law component and the flux-flow component (i.e., $IR'$), which add together to give the simulated $I$-$V$ curve [see Eq. (12)]. The dashed lines show a fit to the apparent power-law region of each curve.

where $\alpha_1$ is temperature dependent with units of $\mathrm{V}/(\mathrm{A})^{a(T)}$, $\alpha_2$ is dimensionless, and $|\alpha_1|$ and $|\alpha_2|$ are of the same order of magnitude.

The expression given by Eq. (12) is perhaps empirically obvious, especially in light of the Ohmic tails present in many $I$-$V$ curves, yet its experimental consequences are often not fully appreciated. Typically, $I$-$V$ power-law behavior is experimentally observable over only one or two decades. The presence of a significant Ohmic tail can easily modify the observed slope of the $I$-$V$ curve, masking the true value of the $I$-$V$ exponent in the power-law region. Figure 5(a) shows the $I$-$V$ curve identified as $T_{a=3}$ for the $W=75$ array, where the dashed line shows a fit to the observed power-law region of the $I$-$V$ curve with a slope of 3. The solid curve is an attempt to reproduce the $I$-$V$ data by adding together a resistive portion (i.e., $IR'$) and the power-law portion ($I^{a(T)}$), both of which are shown as dotted lines. As can be seen, a slope much greater than 3 is needed to reproduce the actual data, meaning that the $I$-$V$ curve experimentally identified as $T_{a=3}$ is actually well below $T_{\mathrm{KT}}$. In Fig. 5(b) we show the $I$-$V$ curve for $T=2.80$ K, and a fit to the observed power-law region (dashed line) yields a slope $a(T)=2.34$. As such, we would normally take this $I$-$V$ curve as being above the KT transition temperature and extract the slope of the lower current region. (That is, we would *not* ignore the Ohmic tail.) A reproduction of the data (solid line), however, requires a power-law slope of approximately 3 (dotted line), meaning that this temperature is actually very near or below $T_{\mathrm{KT}}$. Thus simply extracting the slopes of the observed power-law region of the $I$-$V$ curves will yield incorrect results.

This masking of the power-law exponent will occur whenever a significant Ohmic tail is observed in the $I$-$V$ curve. Slight deviations from power-law behavior, however, should not greatly affect the measured slope. To explore this effect more fully, we used Eq. (12) to produce simulated $I$-$V$ curves for the $W=75$ array, which displays significant $I$-$V$ tails at all temperatures, and for the $W=50$ array, which shows significant deviations from power-law behavior for temperatures near $T_{a=3}$ and only slight deviations for low temperatures. These simulated $I$-$V$ curves are shown in Figs. 6 and 7 where we have also replotted the data Figs. 2(b) and 2(c) to enhance the low-current and low-temperature regimes. The simulated curves (solid lines) show very good qualitative agreement with the data in each case.

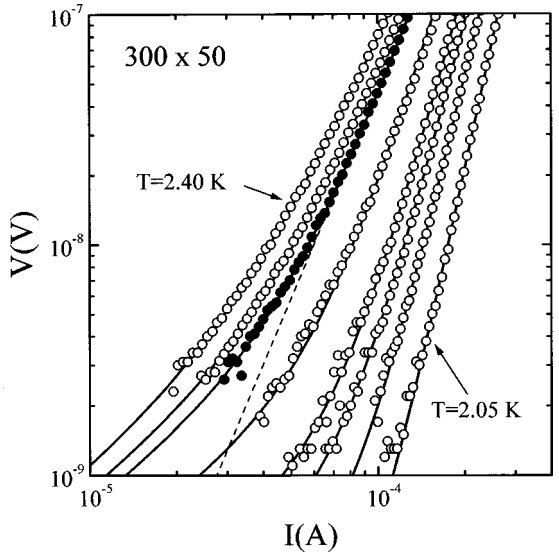


FIG. 6. Current-voltage characteristics for the $W=50$ array. The solid circles denote $T_{a=3}$ (the dotted line shows a slope of 3 fitted to the power-law regime). The solid lines show simulated $I$-$V$ curves as discussed in the text. The unlabeled temperatures are $T=2.35$, 2.32, 2.23, 2.17, 2.14, and 2.10 K, respectively.

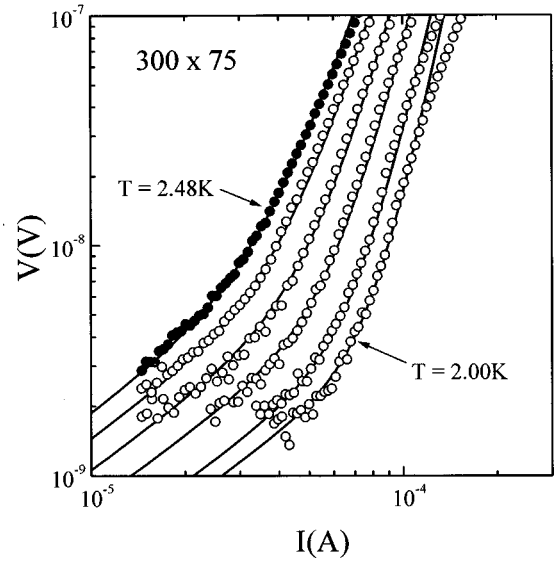


FIG. 7. Current-voltage characteristics for the $W=75$ array. Solid circles denote $T_{a=3}$. Solid lines show simulated $I$-$V$ curves (see text). The unlabeled temperatures are $T=2.40$, 2.30, 2.20, and 2.10, respectively.

It is not surprising that we can fit the data of Figs. 6 and 7 with an equation consisting of the sum of a linear portion and a power-law portion. On closer inspection, however, Eq. (12) is much more restrictive. The exponent $a(T)$ and the free-vortex density $n_f'$ are connected through their mutual dependence on the Josephson coupling energy $E_J$ $[=\hbar i_c(T)/2e]$, which in turn can be expressed in terms of the single-junction critical current $i_c(T)$, a measurable quantity. Thus, by determining $i_c(T)$, we should be able to generate the entire *set* of $I$-$V$ curves which reproduce the features of the $I$-$V$ curves of finite-sized arrays. The KT transition temperature can be determined from the condition that[12] $i_c(T_{\rm KT})/T_{\rm KT} \cong 26.706$ nA/K, leaving only $\beta_0$ [the constant from Eq. (9)] as an adjustable fitting parameter. Once chosen, however, $\beta_0$ remains the same for all $I$-$V$ curves. (The values of $\alpha_1$, $\alpha_2 \approx \log_{10} V/\log_{10} I^{a(T)}$ are extracted from the data at the top of the power-law region of each $I$-$V$ curve and serve only to match the position of the simulated $I$-$V$ curves to the data. They do not otherwise modify the shape of the $I$-$V$ curve.)

The proximity-coupled Josephson junctions of the kind used in our arrays are known to follow the de Gennes expression for the critical current in the dirty limit,[18]

$$i_c(T) = i_c(0)\left(1-\frac{T}{T_{cs}}\right)^2 \exp\left[-\frac{d}{\zeta}T^{1/2}\right], \qquad (13)$$

where $T_{cs}$ is the superconducting electrode transition temperature ($T_{cs}=9.0$ K), $i_c(0)$ is the zero-temperature critical current, $d$ is the junction gap spacing, and $\zeta = [\hbar v_F l/3k_B]^{1/2}$ ($v_F$ is the Fermi velocity, and $l$ is the mean free path). The single-junction critical current $i_c(T)$ is usually extracted from the $I$-$V$ characteristics of an array at temperatures well below $T_{\rm KT}$. For the arrays shown here, $T_{a=3}$ ($\sim T_{\rm KT}$) occurred at temperatures near the lower limit of our experimentally accessible temperature range, making it impossible to extract low-temperature critical current information from the experimental data. We were able to extract the *temperature dependence* of $i_c(T)$ by fitting to the temperature dependence of the measured values of $a(T)$. We then use $i_c(0)$ as a fitting parameter[19] (in addition to $\beta_0$) to yield the best result for the simulated $I$-$V$ curves. We note here that the simulated $I$-$V$ curves shown in Fig. 5 were generated using the same parameters as those in Fig. 7.

We do not wish to overemphasize the importance of the apparent agreement of our simulated $I$-$V$ curves with the data, especially in light of our apparent two-parameter ''fit.'' We do point out, however, that once $i_c(0)$ and $\beta_0$ were determined, the only thing that varied from one $I$-$V$ curve to the other was the temperature.

We now return to the issue of the masking of the $I$-$V$ exponent. Figure 8 shows the measured $I$-$V$ exponents, as obtained by a fit to the power-law portion of the curve, for the $W=50$ array [Fig. 8(a)] and the $W=75$ array [Fig. 8(b)]. The solid lines show the $a(T)$ values used in the simulated $I$-$V$ curves. For the $W=50$ array, a noticeable difference between the measured and simulated values of $a(T)$ exists only for those $I$-$V$ curves with a significant deviation from power-law behavior. For lower-temperature $I$-$V$ curves where the deviation is small, the two values of $a(T)$ are virtually the same. For the $W=75$ array, all of the $I$-$V$ curves

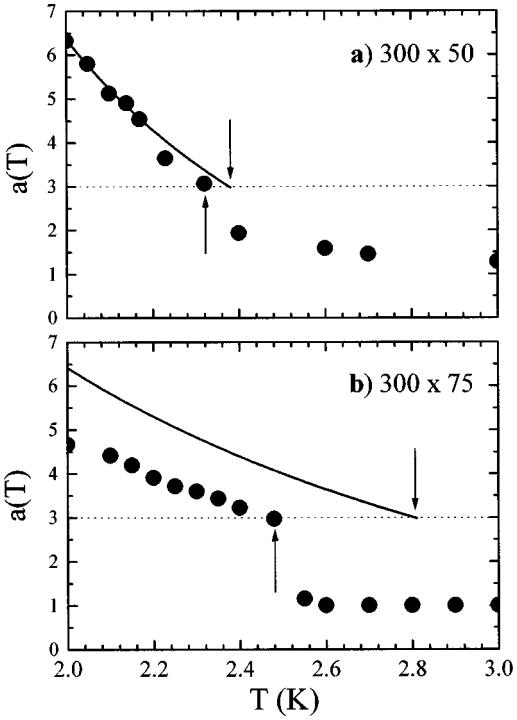


FIG. 8. $a(T)$ vs temperature for (a) the $W=50$ array and (b) the $W=75$ array. Solid circles show data as extracted from the power-law portion of the $I$-$V$ curves. The solid lines represent values used in the simulated $I$-$V$ curves of Figs. 6 and 7.

display a substantial Ohmic tail and the difference between the measured and simulated $a(T)$ values is quite large. The KT vortex-unbinding temperature $T_{\rm KT}$ is given by the temperature at which the simulated $a(T)=3$ since this represents the $I$-$V$ slope for an infinite sample (i.e., one in which the flux-flow resistance due to finite-size-induced free vortices goes to zero). For the $W=75$ array $T_{\rm KT}$ is about 14% higher than $T_{a=3}$, where the measured $a(T)=3$.

The effect of finite-size-induced vortices on the $I$-$V$ curves is embodied in the second term in Eq. (12), which we may label as a finite-size-induced flux-flow resistance $R' = a_0^2 r_n n_f'$. We use this to explore the role that the sample size plays in the appearance of the Ohmic tail. Since it is nearly impossible to fabricate arrays of different sizes with exactly the same coupling energy, we do this by examining the effect that varying the sample size has on simulated $I$-$V$ curves while keeping the coupling energy constant. We start with the same parameters and coupling energy temperature dependence used for the simulated $I$-$V$ curves for the $W=50$ array, and we substitute a width of $W=300$ (instead of $W=50$) for $\mathcal{L}$ in Eq. (9). The corresponding effect (of increasing the sample size) on the $I$-$V$ curves is seen in Fig. 9, where the solid lines are the simulated $I$-$V$ curves for a wider ($W=300$) array, but the data points are the same as shown in Fig. 5 for the $W=50$ array. [We emphasize again that the $W=300$ simulated data shown here is merely an extension of the $W=50$ array to a larger width and is not to be confused with the $W=300$ array data shown in Fig. 2(a), which has a different coupling energy.] Note that the Ohmic tail for $T_{a=3}$ ($=2.32$ K) in the simulated wider array (solid line) is practically nonexistent.

Notice, also, in Fig. 9 that the lowest-temperature simu-

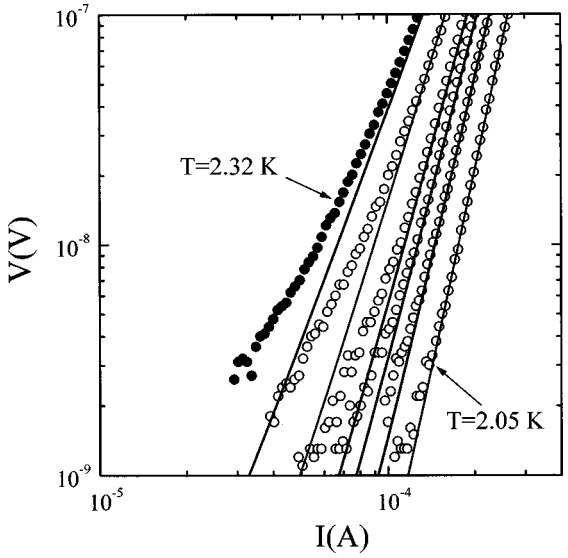


FIG. 9. $I$-$V$ curves illustrating the effect of finite size at constant coupling strength. The solid lines are $I$-$V$ curves using the hypothetical $R'$ for an array 300 crosses wide ($r_n = 26\ \mathrm{m}\Omega$). Open circles show data for the $W = 50$ array as shown in Fig. 2(c).

lated $I$-$V$ curve shows little effect of increasing the sample width. This is the result of $n_f'$ being dependent on $\mathcal{L} = \min(L, \lambda_\perp)$; as the temperature is lowered, $i_c(T)$ increases and $\lambda_\perp$ [$\propto 1/i_c(T)$] decreases, eventually becoming smaller than $L$. Thus, below a certain temperature, all arrays with the same coupling-energy temperature dependence, regardless of their size, will have a similar resistive tail. This implies that simply fabricating much larger arrays will not necessarily decrease the number of finite-size-induced vortices. Larger arrays mean that $\lambda_\perp$ will become smaller than the sample size at a higher temperature. Only in making very weakly coupled large arrays, so that $\lambda_\perp$ remains relatively large at low temperatures, can the number of finite-size-induced free vortices be reduced so that we will observe $I$-$V$ curves with no Ohmic tail below $T_{\mathrm{KT}}$.

The actual shape, then, of the $I$-$V$ characteristics in Josephson junction arrays depends in a complicated way on the array size and coupling-energy temperature dependence. The $W = 75$ array has a relatively weak temperature dependence and, because it is narrow, has a large finite-size-induced free-vortex Ohmic tail. Consequently, the true slope of the $I$-$V$ curve is masked and the nominal vortex-unbinding temperature occurs well above the temperature at which an $I$-$V$ curve with a measured slope of 3 is observed. On the other hand, the $W = 50$ array has a smaller resistive tail than the $W = 75$ array, even though it is narrower, because its much stronger coupling-energy temperature dependence causes the free-vortex density to decrease more precipitously. The result is that a measured slope of three occurs very near to the nominal vortex-unbinding temperature. This complex dependence on coupling strength is one reason why in the $W = 50$ array the Ohmic tail disappears more quickly with temperature and is less noticeable than for the $W = 75$ array.

The masking of the power-law exponent may call into question the validity of our method of determining $i_c(T)$ from the temperature dependence of $a(T)$. In the case of the $W = 50$ array, the coupling-energy temperature dependence is sufficiently strong that only $I$-$V$ curves very near $T_{\mathrm{KT}}$ have an appreciable Ohmic tail and thus have a power-law exponent that is appreciably masked. $I$-$V$ curves well below $T_{\mathrm{KT}}$ are only slightly modified, and the measured values of $a(T)$ should be very close to the nominal values. Fitting to the low-temperature measured values should yield the actual temperature dependence of $a(T)$. (The results of the simulated $I$-$V$ curves of Fig. 6 seem to bear this out.) In the case of the $W = 75$ array, the coupling-energy temperature dependence, and consequently the temperature dependence of $R'$, is sufficiently weak that all measured $I$-$V$ curves are modified by the presence of an Ohmic tail in a similar way, and thus the temperature dependence of $a(T)$ is preserved. One can imagine an intermediate case, however, in which the masking of $a(T)$ is highly temperature dependent. In such a case (and, indeed, as a general case), the temperature dependence of the coupling energy could not be extracted from the measured values of $a(T)$ and $i_c(T)$ would need to be determined independently.

## VII. SUMMARY

Any finite-sized array will have free vortices present at all nonzero temperatures. The actual number of free vortices, and the corresponding effect on the electrical transport properties of the array, depends in a complex manner on the size of the array and the coupling-energy temperature dependence. The appearance of an Ohmic tail in $I$-$V$ curves at and below $T_{\mathrm{KT}}$, in the form of a deviation from pure power-law behavior at low currents, is a clear indication that the presence of free vortices cannot be neglected and that the KT transition is not strictly observed. In addition, the existence of an Ohmic tail in $I$-$V$ curves at and below $T_{\mathrm{KT}}$ means that the power-law exponent may be significantly modified from its nominal value. As such, the measured values of $a(T)$ will not give a true picture of vortex unbinding and further analysis may be required. These results will apply to other finite 2D systems, such as superconducting granular films and high-temperature cuprate superconductors, so that care must be taken when analyzing $I$-$V$ curves.

*Note added in proof:* Simkin and Kosterlitz have recently examined the issue of finite-size effects in arrays using renormalization group analysis and numerical simulation. Their results are consistent with those shown here.[20]

## ACKNOWLEDGMENTS

We wish to acknowledge Edward Harris and Richard Bojko for their assistance in fabricating the arrays. This work was supported in part by grants from the ONR under Contract No. 00014-92-J-1686 (Cincinnati), from the Air Force under Grant No. F49620-92-J-0041 (Maryland), and by the Cornell Nanofabrication Facility.

## APPENDIX

For a rectangular array of length $L$ and width $W$ (both in units of the array lattice constant $a_0$), we may use a simple thermodynamic argument to obtain a *rough* estimate of the critical width for which an array crosses over from two- to one-dimensional behavior. An array will exhibit one-

dimensional behavior when thermal fluctuations cause an entire row of width $W$ to phase slip. The change in energy for this event will be $\Delta E_{\mathrm{row}} = W(2E_J)$, and the entropy associated with a row phase slipping is $\Delta S_{\mathrm{row}} = k_B \ln(L)$. The change in the free energy of the array for this process is thus

$$\Delta F_{\mathrm{row}} = 2WE_J - k_B T \ln(L). \tag{A1}$$

For our purposes we may approximate $E_J \approx (2/\pi) k_B T_{\mathrm{KT}}$ so that

$$\Delta F_{\mathrm{row}} = W \frac{4}{\pi} k_B T_{\mathrm{KT}} - k_B T \ln(L). \tag{A2}$$

If we let $W = L \to \infty$, we see that $\Delta F_{\mathrm{row}}$ is always greater than zero; hence, this event will not occur. For finite samples, however, there will exist some crossover temperature $T_{\mathrm{row}}$, such that for $T > T_{\mathrm{row}}$, the array will exhibit large numbers of row switching events (1D behavior), while for $T < T_{\mathrm{row}}$, there will be relatively few row switching events (2D behavior). If we set $\Delta F_{\mathrm{row}} = 0$, Eq. (A2) becomes

$$W = \left(\frac{T_{\mathrm{row}}}{T_{\mathrm{KT}}}\right) \frac{\pi}{4} \ln(L) = 4.5 \left(\frac{T_{\mathrm{row}}}{T_{\mathrm{KT}}}\right), \tag{A3}$$

where the second expression comes from substituting $L = 300$ for our arrays. If $T_{\mathrm{row}} \gg T_{\mathrm{KT}}$, the array will appear two dimensional, while if $T_{\mathrm{row}} \ll T_{\mathrm{KT}}$, the array will appear one dimensional. Setting $T_{\mathrm{row}} = T_{\mathrm{KT}}$, we obtain $W = 4.5$ as a rough estimate of the width of the array for which the crossover from 2D to 1D behavior occurs. This value will be modified slightly by the renormalization of the vortex interaction. In Eq. (A1), we should have used the renormalized coupling energy $E_J^* = E_J / \epsilon_c$, resulting in an increase in the estimated value of the crossover width by a factor of $\epsilon_c$. As $\epsilon_c$ is typically on the order of 2 for arrays, this would result in an approximate doubling of the previous estimate. This compares favorably with the observed width of $W = 15$.

*Present address: J&L Tech. Co., LTD. Seoul, Korea.
†Permanent address: Department of Physics, Ajou University, 5 Wonchun-Dong Kwon, Suwon, Kyunggi-do, 441-749, Korea.

[1] M. R. Beasley, J. E. Mooij, and T. P. Orlando, Phys. Rev. Lett. **42**, 1169 (1979).
[2] J. Pearl, Appl. Phys. Lett. **5**, 65 (1964).
[3] D. J. Resnick, J. C. Garland, J. T. Boyd, S. Shoemaker, and R. S. Newrock, Phys. Rev. Lett. **47**, 1542 (1981); A. F. Hebard and A. T. Fiory, *ibid.* **44**, 291 (1980); K. Epstein, A. M. Goldman, and A. M. Kadin, *ibid.* **47**, 534 (1981); D. W. Abraham, C. J. Lobb, M. Tinkham, and T. M. Klapwijk, Phys. Rev. B **26**, 5268 (1982).
[4] See, for instance, N-C. Yeh and C. C. Tsuei, Phys. Rev. B **39**, 9708 (1989); S. Martin, A. T. Fiory, R. M. Fleming, G. P. Espinosa, and A. S. Cooper, Phys. Rev. Lett. **62**, 677 (1989); Q. Y. Ying and H. S. Kwok, Phys. Rev. B **42**, 2242 (1990).
[5] J. M. Kosterlitz and D. J. Thouless, J. Phys. C **6**, 1181 (1973); V. L. Berezinskii, Sov. Phys. JETP **34**, 610 (1972).
[6] Petter Minnhagen, Rev. Mod. Phys. **59**, 1001 (1987).
[7] Y. Jun, S. T. Herbert, K. Ravindran, D. B. Mast, and R. S. Newrock (unpublished).
[8] B. I. Halperin and David R. Nelson, J. Low Temp. Phys. **36**, 1165 (1979).
[9] S. Doniach and B. A. Huberman, Phys. Rev. Lett. **42**, 1169 (1979).
[10] D. C. Harris, S. T. Herbert, D. Stroud, and J. C. Garland, Phys. Rev. Lett. **67**, 3606 (1991); D. C. Harris, Ph.D. thesis, Ohio State University, 1989.
[11] J. M. Repaci, C. Kwon, Qi Li, Xiuguang Jiang, T. Venkatessan, R. E. Glover, R. S. Newrock, and C. J. Lobb, Phys. Rev. B **54**, R9674 (1996).
[12] C. J. Lobb, D. W. Abraham, and M. Tinkham, Phys. Rev. B **27**, 150 (1983).
[13] A. M. Kadin, K. Epstein, and A. M. Goldman, Phys. Rev. B **27**, 6691 (1983).
[14] J. M. Repaci and C. J. Lobb (unpublished). (In fact, $\beta_0$ may depend on the applied current, though in most cases this dependence is very weak.)
[15] V. Ambegaokar, H. Halperin, D. Nelson, and E. Siggia, Phys. Rev. Lett. **40**, 783 (1978).
[16] P. Minnhagen, O. Westman, A. Jonsson, and P. Olsson, Phys. Rev. Lett. **74**, 3672 (1995).
[17] S. T. Herbert, Y. Jun, L. B. Gomez, S. Elhamri, K. Ravindran, D. B. Mast, and R. S. Newrock (unpublished).
[18] P. D. de Gennes, Rev. Mod. Phys. **36**, 225 (1964).
[19] Practically speaking, any particular measurement technique consistently underestimates or overestimates the value of $i_c(T)$; thus, it is difficult to determine the precise value of $i_c(0)$ by measurement in any case.
[20] M. V. Simkin and J. M. Kosterlitz, Phys. Rev. B **55**, 11 646 (1997).